Enhanced Condensation for Organic Rankine Cycle

5th Quarterly Progress Report

Reporting Period: January 1, 2014 – April 30, 2014

Project Grantor: **Alaska Energy Authority**
Alan Baldivieso, Program Manager
813 W. Northern Lights Blvd. AK 99503
907-771-3027 (voice), Email: abaldivieso@aidea.org

Project Grantee: University of Alaska, Institute of the Northern Engineering
Maggie Griscavage
P.O. Box 757880, Fairbanks, AK 99775
907-474-7301 (voice), Email: fygrcon@uaf.edu\

Grant Agreement Number: 7310028
Project Code: 413006

Principal Investigators: **Sunwoo Kim**, PhD (PI)
Mechanical Engineering Department
University of Alaska, Fairbanks
907-474-6096 (voice), Email: swkim@alaska.edu

1. Back Ground

Generating electricity from low grade heat sources has attracted attention due to rising fuel price and increasing energy demand. The organic Rankine cycle (ORC) system is the most practical solution among technologies developed for low grade heat recovery. However, the efficiency of a typical small scale ORC is 10% or less. Most energy loss in the ORC is attributed to thermodynamically irreversible heat transfer processes occurring in its heat exchangers: the evaporator and condenser. In particular for waste heat recovery ORCs, economical success is mainly determined by effectiveness of the condenser because, while their heat source is provided at no cost, heat rejection accounts for most of operation cost. Almost half of total cost for operation and maintenance of an ORC system can stem from its condenser. We investigate and demonstrate heterogeneous condensing surfaces that potentially reduce the irreversibility during the condensation of organic fluids.

2. Progress Report

We have made progress during the reporting period (January 1 – April 30, 2014) and progress activities are described below.

Task 1: Model Development (Completed)

Task 2: Design and Construction of Testing Apparatus (Completed)

The condensation apparatus has been constructed and is in fully operational condition.

Some minor modifications and improvements were continuously made, including the installation of a thermocouple in the vicinity of the condensing surface. Figure 1 shows the copper block, which plays a role of heat path between the vapor in the condensing chamber and the coolant in the cooling chamber. A groove (0.01 inches wide, 0.01 inches deep and 0.75 inches long) was machined on the copper block's surface to incorporate a type J thermocouple to measure the surface temperature of the copper. The groove is photographed in the Figure 2. In the picture the copper rod sitting flush to the stainless steel disk is shown.

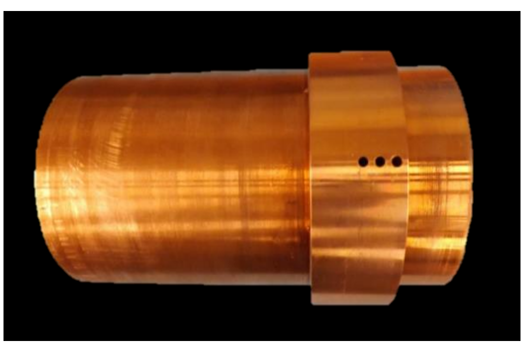

Figure 1: Photograph of the copper block

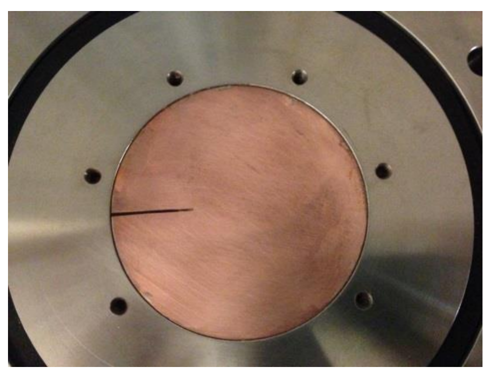

Figure 2: A groove on side of the copper block

Task 3: Initial Performance Testing

Initial performance tests continued during the reporting period. All experimental conditions and method were set to be the same as the previous experiments except that we made a comparison between a plain copper condensing surface and a hydrophobic-treated sample.

<u>Plain copper condensing surface</u>

The condensation on the plain copper sample was first observed at different subcooling temperatures (the difference between the vapor saturation temperature and the condensing surface temperature) to provide a baseline. The mode of condensation was dropwise. The formation of the drops and the coalescence of the drops were visually studied. The sliding of the coalesced drops away from the plain copper sample and the movement of other drops in the process of sliding were slower at smaller subcooling temperatures than at larger subcooling temperatures. The number of drops formed at the smaller subcooling temperature was noticeably less when compared to that at larger subcooling temperature. Consequently, the area of the plain copper sample exposed directly to the vapor appeared greater when the subcooling temperature was relatively small. The drops did not depart on the surface until they reached about 6 mm in diameter.

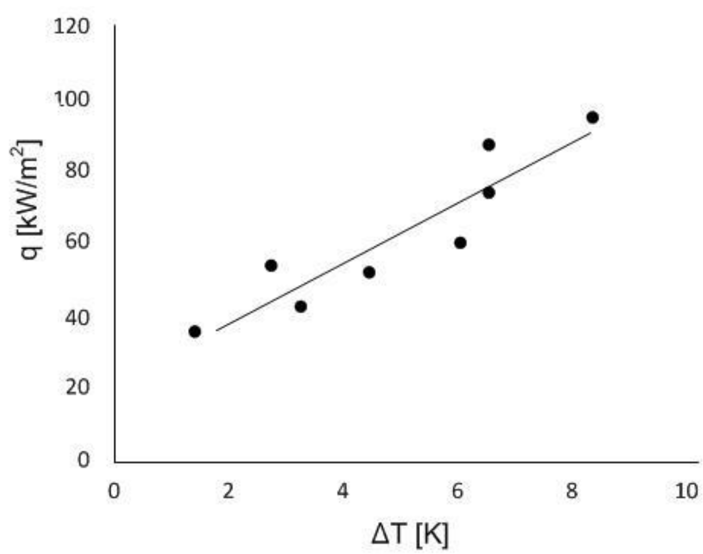

Figure 3: Heat flux for the plain copper sample

Figure 3 shows the heat flux with the variation of the subcooling temperature. It is observed that the heat flux increases with the subcooling temperature. This result accords with the visual observation that the rate of drop falling from the surface was higher at higher subcooling.

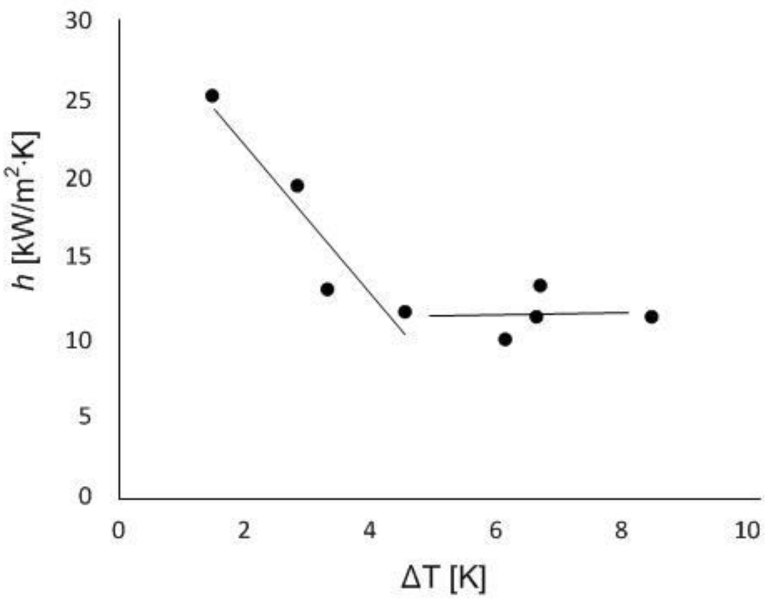

Figure 4: Heat transfer coefficient for the plain copper sample

The condensation heat transfer coefficient on the plain copper sample is plotted for the subcooling temperature ranging 1 to 10 K in Fig. 4. The graph can be divided into two sections: one with a steep declination at low subcooling temperatures and the other with a flat trend line. The least square regression method is employed to generate trend lines for this graph. Steep declination is observed in subcooling temperatures from 1 to 4 K. In this range of subcooling temperatures, the formation of the drops was at the beginning stage. Thus, the plain copper surface allowed more surface area that was exposed directly to the vapor, because there formed a less number of drops on it. As a result, the overall resistance to the heat transfer from the vapor to the surface remained low. The graph reflects that the overall thermal resistance increases significantly with the subcooling temperatures up to 4 K (the overall thermal resistance is inversely proportional to the heat transfer coefficient). In the subcooling range of 1 to 4 K, the number of drops formed on the plain copper sample gradually increased with the increase in the subcooling due to direct condensation. This explains the steep declination of the heat transfer coefficient.

The transition of the trend occurs at the subcooling temperature 4 K. As shown by the second trend line representing h's for $\Delta T > 4$ K, the heat transfer coefficient remained at around 12 kW/m^2-K after the transition. With an increase in ΔT, the rate of condensation proportionally increases. When $\Delta T = 4$ K, however, the total volume of droplets on the surface no longer escalated because of the rapid sweeping by falling drops. Therefore, the overall thermal resistance was kept nearly constant, leading to the flat trend of the heat transfer coefficient h.

Hydrophobic copper condensing surface

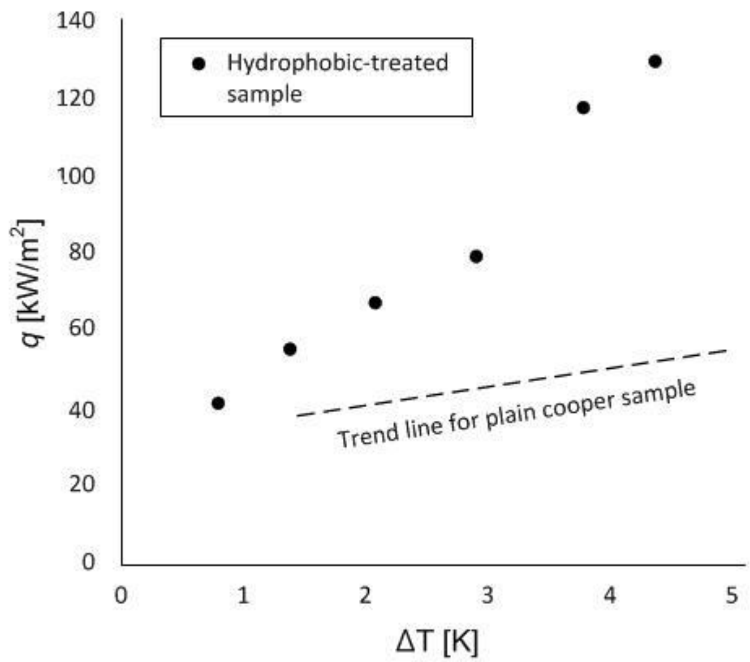

Figure 5: Heat flux for the hydrophobic sample

The hydrophobic-treated sample outperformed the non-treated plain sample. Fig. 5 displays the heat flux measured on the hydrophobic-tread sample in comparison with the plain sample. No signs of film condensation were observed as expected. The average diameter of departing drops was visually measured around 3 - 4 mm. This meant that the size of departing drops was smaller by 2 mm than that on the plain sample. The cause of this difference lies in the wettability. Whereas the drops on a greater wettability do not start moving until they are heavy enough, ones on hydrophobic surface depart and clean off other drops on its path at less weight. The experimental results obviously reflect this in Fig. 5. The hydrophobic surface generated heat fluxes almost twice as much as the plain copper sample, which is represented by the dotted line. This is improvement is significant in that both the plain and hydrophobic samples promoted dropwise condensation. Even, visually examined contact angles were found almost identical on the both surfaces.

A data pattern similar to in Fig. 4 is viewed in Fig. 6 that shows the heat transfer coefficient on the hydrophobic-treated surface with respect to the subcooling temperature. This graph also can be divided into two parts, but for the hydrophobic surface, transition takes place at the subcooling temperature of 2 K. The same reasoning can be adopted to explain the variation of h; the curve before $\Delta T = 2$ K has a steep slope and after there it is flat. For the plain copper, sample the transition in the curve takes place at $\Delta T =$ 4. This implies that the moment when the total volume of drops on the condensing surface stops rising is reached at lower subcooling when hydrophobicity of the condensing surface is reinforced. According to our visual observation, the size of departure drops was smaller on the hydrophobic surface. A less population of large drops resulted in a smaller total volume of drops and consequently a decrease in the overall thermal resistance, which caused the rise of the heat transfer coefficient h. At $\Delta T = 1$ K, *h* for the hydrophobic-treated copper sample was approximately 50 kW/m^2-K while that for the plain copper sample about 25 kW/m^2-K. Even at their respective transition temperatures, the h for the hydrophobic-treated copper sample was twice.

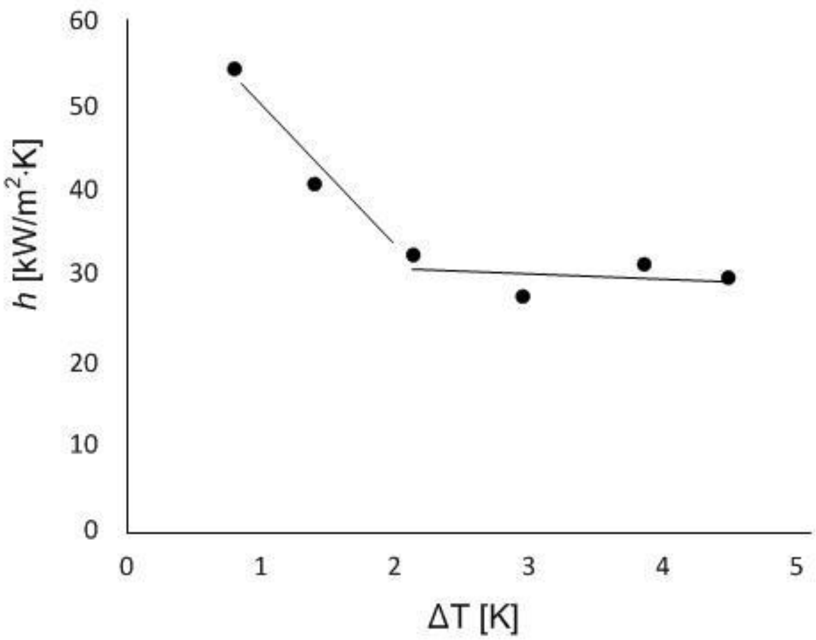

Figure 6: Heat transfer coefficient for hydrophobic sample

The uncertainty of the heat transfer coefficient ($\delta h/h$) can be determined by the standard approach presented by Coleman and Steele (1999).

$$\frac{\delta h}{h}=\left[\left(\frac{\delta T_{st}}{T_{st}}\right)^2+\left(\frac{\delta T_s}{T_s}\right)^2+\left(\frac{\delta h_c}{h_c}\right)^2+\left(\frac{\delta q}{q}\right)^2\right]^{1/2}$$

where h is the heat transfer coefficient, T_{st} is the steam temperature, T_s is the surface temperature, q is the average heat flux, and h_c is the thermal contact conductance. For thermocouples, ($\delta T/T$) is given by the manufacturers and the value is approximately 0.75%. For calculation of the thermal contact resistance, we assumed the thermal contact conductance of the copper to copper contact to be 200,000 W/m^2-K. This value is chosen from the range of values given in the literature (Cengel and Ghajar, 2010). For $\delta h_c/h_c$, the maximum uncertainty that is possible so that $T_s < T_{st}$ is calculated 3%. The uncertainty of the average heat flux is calculated by using higher-order uncertainty principle as explained by Figliola and Beasley (1991). The uncertainty of the average heat flux ($\delta q/q$) is 3.74%. From the equation, the uncertainty of the measurement of the heat transfer coefficient is $\delta h/h$ =4.68%.

Task 4: Optimization of design parameters

One of the project main objectives is to evaluate the performance of a heterogeneous condensing surface in comparison with a plain copper sample, a hydrophobic-treated copper sample. The heterogeneous sample is a copper disk, on one side of which parallel stripes are patterned such that ones with hydrophobic feature and ones without it alternate. In contrast, on the hydrophobic sample, the same hydrophobic treatment is applied on the entire condensing surface, instead of alternating with non-treated stripes. The test samples are 3-inches in diameter and 0.031 inches in thickness. These samples are attached to the heat conduction rod by using a thermal paste whose thermo physical properties are known (given by the manufacturer). As described in the previous section, we tested a plain copper sample, where no treatment was done. In order to prepare the hydrophobic and heterogeneous samples, plain copper disks were sent to NEI Corporation, who treated the copper samples with their hydrophobic formula. The chemical composition and thickness of the hydrophobic coating were not revealed to us.

The heterogeneous sample was prepared through machining the hydrophobic samples in such a way that the sample has alternative hydrophobic layers and copper substrate layers, as shown in Fig 7. For removal of the hydrophobic coating layer, a precise milling machine was used. The machine minimum cutting thickness of 25.4 μm was sufficient to clearly mill the coating, showing that the thickness of coating is thinner than the cutting thickness. The dark region stands for the hydrophobic surface and the light region the bare copper. All the dimensions shown in the figure are in inches.

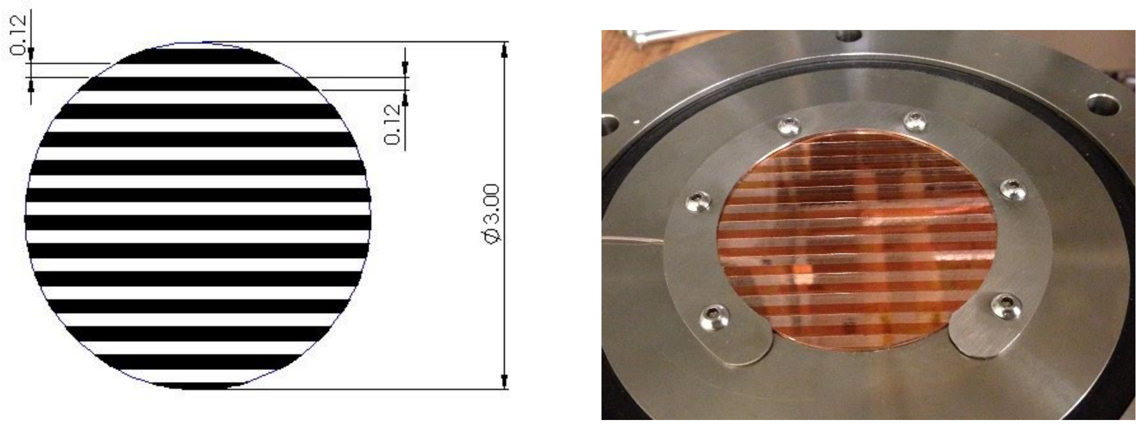

Figure 7: Heterogeneous condensing surface
(left: design, right: photograph when it is attached in the condensation apparatus)

References

1. Coleman, H.W., and Steele, W.G.., 1999, *Experimentation and uncertainty analysis for engineers*, Wiley
2. Cengel, Y., and Ghajar, A., 2010, *Heat and mass transfer: Fundamentals and Applications*, McGraw-Hill Education.